Multihydroxy Polymer-Functionalized Carbon Nanotubes: Synthesis, Derivatization, and Metal Loading

Chao Gao,*,†,§ Cong Duan Vo,‡ Yi Zheng Jin,§ Wenwen Li,† and Steven P. Armes*,‡

College of Chemistry and Chemical Engineering, Shanghai Jiao Tong University, 800 Dongchuan Road, Shanghai 200240, P. R. China; Department of Chemistry, Dainton Building, University of Sheffield, Brook Hill, Sheffield, S3 7HF, UK; and Nanoscience and Nanotechnology Centre, Department of Chemistry, School of Life Sciences, University of Sussex, Brighton BN1 9QJ, UK

Received April 19, 2005; Revised Manuscript Received August 15, 2005

ABSTRACT: Multiwalled carbon nanotubes (MWNTs) were oxidized with concentrated HNO_3 and H_2SO_4 to introduce carboxylic groups onto MWNT surfaces. The oxidized MWNTs were reacted subsequently with thionyl chloride, glycol, and 2-bromo-2-methylpropionyl bromide, producing MWNT-based macroinitiators, MWNT-Br, for the atom transfer radical polymerization (ATRP) of glycerol monomethacrylate (GMA). In the presence of *N*,*N*,*N*′,*N*″,*N*″-pentmethyldiethylenetriamine (PMDETA)/Cu(I)Br, hydroxyl-functional polyGMA, with weight concentration of ca. 50−90%, was successfully grown from the MWNT surface. Comparative experiments, with MWNT-Br and ethyl 2-bromoisobutyrate as co-initiators, showed that (1) the presence of free initiator has no significant effect on the nanotube-surface initiating polymerizations, (2) both the polymer content grafted on the nanotubes (46−88 wt %) and the number-average molecular weight (M_n) of free polymer (3000−17 000) can be efficiently controlled by adjusting the feed ratio of monomer to co-initiators, and (3) the polydispersity index (PDI) of the free polymer increased when either the feed ratio or the molecular weight was increased. Further derivatization of the grafted polyGMA with succinic anhydride converted the hydroxyl groups into carboxylic acid groups. The resulting polymer-functionalized MWNTs were characterized with FTIR, ^{1}H NMR, ^{13}C NMR, TGA, SEM, and TEM. Furthermore, the poly(carboxylic acid)-modified MWNTs were used to sequester metal ions such as Ag^+, Co^{2+}, Ni^{2+}, Au^{3+}, La^{3+}, and Y^{3+}, forming MWNT-polymer/metal hybrid nanocomposites, nanowires, or necklace-like nanostructures, depending on the grafted polymer content and the nature of the captured metal. SEM and TEM studies combined with X-ray analyses confirmed the structure and elements of the novel hybrid nanoobjects. Interestingly, polymer enwrapped-silver nanobeads or nanodots with a diameter of ca. 3−10 nm decorating the convex surface of MWNTs were obtained. The synthesis, derivatization, and metal loading of functionalized MWNTs suggests a new route for rational molecular design and augurs well for future applications of functionalized nanomaterials, including device fabrication.

Introduction

Functionalization or modification of carbon nanotubes (CNTs)[1] has become a major activity within the interdisciplinary fields of nanoscience, nanotechnology, bioengineering, and bionanotechnology, as it promises to be the best approach for improving the solubility and compatibility of CNTs, tailoring the structure and properties of CNTs, and preparing novel CNT-based nanodevices, nanocomposites, and bionano complexes or adducts.[2] In this regard, the combination of CNTs with macromolecules is of particular interest as a desirable and facile route to improve the conventional polymer properties or to obtain new nanomaterials.[3] Such CNT/polymer nanocomposites can be accessible through the methodologies of noncovalent mixing/adsorption and covalent linkage.[4,5] Generally, covalent functionalization makes the resulting composites more stable and more controllable.[6]

So-called "grafting to" and "grafting from" approaches have been employed to prepare CNT−polymer adducts or hybrids. The "grafting to" route involves attaching as-prepared or commercially available macromolecules onto the CNT walls and ends by amidation, esterification, radical coupling, or other reactions, followed by removal of unreacted polymers by filtering or centrifuging. A prerequisite of this approach is that the macromolecules must possess suitable reactive functional groups or radicals. Hitherto, many linear polymers such as polystyrene (PS),[7,8] poly(sodium 4-stryrenesulfonate),[9] poly(methyl methacrylate) (PMMA),[10] polyimide,[11] poly(2-vinylpyridine),[12] poly(propionylethylenimine-*co*-ethylenimine (PPEI-EI),[13] oligomeric and polymeric species containing poly(ethylene glycol) (PEG) blocks,[5,14] poly(vinyl alcohol) (PVA) and its related copolymer poly(vinyl acetate-*co*-vinyl alcohol) (PVA-VA),[15] and poly(*m*-aminobenzenesulfonic acid) (PABS)[16] as well as dendrons,[17] dendrimers,[18] and hyperbranched polymers[19] were successfully bonded onto CNTs. Generally, the grafted polymer content is quite limited due to the relatively low reactivity of macromolecules.[19] In contrast, the "grafting from" approach, which involves growing polymers from CNT surfaces by the in situ polymerization of monomers in the presence of reactive CNTs or CNT-supported macroinitiators, makes efficient, controllable grafting feasible. This strategy has been used to graft various linear polymers such as PS,[7,20,21] PMMA,[6,21−23] poly(sodium 4-stryrenesulfonate),[24] poly(acrylic acid) (PAA),[24] poly(2-hydroxyethyl methacrylate) (PHEMA),[6] poly(*n*-butyl methacrylate),[25] poly(*tert*-butyl acrylate),[24,26] poly(*N*-isopropylacrylamide),[27,28] poly(4-vinylpyridine),[29] and poly(*N*-vinylcarbazole)[30] as well as hyperbranched poly(3-ethyl-3-hydroxymethyloxetane)[31] and poly(amidoamine)[19] onto CNT surfaces

† Shanghai Jiao Tong University.
‡ University of Sheffield.
§ University of Sussex.
* To whom correspondence should be addressed. C. Gao: tel +86-21-5474 2665; fax +86-21-5474 1297; e-mail chaogao@sjtu.edu.cn. S. P. Armes: e-mail: S.P.Armes@sheffield.ac.uk.

10.1021/ma050823e CCC: $30.25
Published on Web 09/17/2005

via radical, cationic, anionic, ring-opening, and condensation polymerizations. After grafting, the resulting polymer−CNT nanohybrids exhibit good solubility and dispersibility in solvents, especially at high polymer loadings. In these cases, the CNTs are often reduced to several microns or a few hundred nanometers in length and can be separated from each other individually. Therefore, individual core−shell nanocables with a cylindrical core of nanotube and a shell of polymer layer can be obtained. There is no doubt that this covalent functionalization of CNTs opens up new opportunities for the design, synthesis, and application of CNT-based nanomaterials and nanodevices. Unfortunately, most examples of tethered polymers have few or no functional groups, which restricts their further derivatization.

In this work a highly hydrophilic water-soluble polymer, poly(2,3-dihydroxypropyl methacrylate), was attached to CNT convex surfaces by the "grafting from" approach. 2,3-Dihydroxypropyl methacrylate, also known as glycerol monomethacrylate (GMA), is a functional speciality monomer of both academic and commercial interest. It has been used to prepare biocompatible amphiphilic networks and soft contact lenses.[32,33] Thus, it would be fascinating if such a biocompatible polymer can be grafted onto CNTs since the high density of hydroxyl groups and the tubular nanostructure provide a versatile platform to design and construct novel nanoobjects.

Furthermore, Armes and co-workers[34] have shown that GMA can be easily controllably polymerized at ambient temperature by atom transfer radical polymerization (ATRP),[35] a powerful living/controlled polymerization tool in the preparation of functional (co)polymers and modification of surfaces. Therefore, we evaluated ATRP in order to graft polyGMA onto CNTs. To explore potential applications of these polyGMA-functionalized CNTs, we further derivatized the hydroxyl groups into carboxylic acids. The resulting polyacid-coated CNTs were used to sequester metal ions and hence to prepare novel CNT-polymer/metal hybrid nanocomposites and nanowires.

Experimental Section

Materials. The multiwalled carbon nanotubes (MWNTs) made from the chemical vapor deposition method were purchased from Tsinghua-Nafine Nano-Powder Commercialization Engineering Centre in Beijing (>95% purity). Glycerol monomethacrylate (GMA) monomer (92% purity; the remaining 8% is the 1,3-dihydroxyisopropyl methacrylate isomer) was kindly donated by Röhm (Germany) and used as received. Cu(I)Br (99.999%), 2-bromo-2-methylpropionyl bromide (α-bromoisobutyryl bromide, 98%), ethyl 2-bromoisobutyrate (98%), glycol ($HOCH_2CH_2OH$, ≥99%), succinic anhydride (≥99%), thionyl chloride ($SOCl_2$, ≥99%), *N*,*N*,*N*′,*N*″,*N*″-pentmethyldiethylenetriamine (PMDETA, 99%), *N*,*N*-(dimethylamino)pyridine (DMAP, ≥99%), triethylamine (≥99%), tetrahydrofuran (THF, ≥99%), *N*,*N*-dimethylformamide (DMF, ≥99.8%), dimethyl sulfoxide (DMSO, ≥99.9%), acetone (≥99.5%), methanol (≥99.8%), ethanol (≥99.5%), chloroform ($CHCl_3$, ≥99.8%), $AgNO_3$ (99.9999%), $Co(NO_3)_2$ (99.999%), $Ni(NO_3)_2$ (99.999%), $La(NO_3)_3$ (99.999%), $Y(NO_3)_3$ (99.9%), and all other reagents or solvents were purchased from Aldrich (unless otherwise stated) and were used as received.

Characterization and Instrumentation. Fourier transform infrared (FTIR) spectra were recorded on a PE Paragon 1000 spectrometer using the KBr disk method. Nuclear magnetic resonance (^1H 500 MHz or ^{13}C 125 MHz NMR) spectra were measured in DMSO-d_6 with a Bruker 500 MHz spectrometer. Molecular weights and polydispersities of the polymers were measured by gel permeation chromatography (GPC). The GPC setup consisted of three Polymer Laboratories PL gel 5 μm Mixed "B" columns kept at a temperature of 70 °C and an RI detector. The GPC eluent was HPLC grade DMF containing 0.01 M LiBr with the flow rate of 1 mL min^{-1}. Calibration was carried out using poly(methyl methacrylate) (PMMA) standards. Thermogravimetric analyses (TGA) were conducted on a PE TGA-7 instrument at a heating rate of 20 °C min^{-1} under nitrogen. Transmission electron microscopy (TEM) studies were performed on either a Hitachi H7100 electron microscope operating at 100 kV or a JEOL JEM 2200FS electron microscope (equipped with a JEOL electron diffraction (ED) analyzer and an energy dispersive spectrometer (EDS)) operating at 200 kV, respectively. Scanning electron microscopy (SEM) images and relevant elemental analysis were recorded using a LEO-5000 microscope equipped with an Oxford EDS analyzer operating at 10 kV, and the samples of solid powder were loaded on the carbon film substrate. Raman spectra were recorded on a LabRam-1B Raman spectroscope operating at a laser wavelength of 632 nm.

Synthesis of MWNT-COOH. Carboxyl-functionalized multiwalled carbon nanotubes (MWNT-COOH) can be prepared by oxidation of pristine MWNTs with ca. 60% HNO_3 for around 24 h under reflux as described previously.[6,20] Here, we used concentrated H_2SO_4/HNO_3 (3:1 by volume) as the oxidant to prepare MWNT-COOH. This procedure only needs 1−3 h. A specific example is given as follows.

Into a 1000 mL flask equipped with a condenser, pristine MWNTs (12.0 g, 1.0 mol C), HNO_3 (65%, 100 mL, 1.465 mol), and H_2SO_4 (98%, 300 mL, 5.52 mol) were added with vigorous stirring. The flask was then immersed in an ultrasonic bath (40 kHz) for 10 min. The mixture was then stirred for 100 min under reflux (the oil bath temperature was increased gradually from 90 to 133 °C). A dense brown gas was evolved during this period, which was collected and treated with aqueous NaOH connected to the condenser by a plastic tube. After cooling to room temperature, the reaction mixture was diluted with 500 mL of deionized water and then vacuum-filtered through a filter paper (Fischer). The solid was dispersed in 500 mL of water and filtered again, and then 200 mL of water was used to wash the filter cake several times. The dispersion, filtering, and washing steps were repeated until the pH of the filtrate reached 7 (at least four cycles were required). The filtered solid was then washed with ca. 200 mL of acetone and THF five times to remove most of the water from the sample and dried under vacuum for 24 h at 60 °C, giving 7.2 g (~60% yield) of MWNT-COOH.

Synthesis of MWNT-OH and MWNT-Br. The as-prepared MWNT-COOH (2.0 g) was reacted with excess neat $SOCl_2$ (50 mL, 0.685 mol) for 24 h under reflux (the temperature of oil bath was 65−70 °C). The residual $SOCl_2$ was removed by reduced-pressure distillation equipped with a liquid nitrogen trap, giving acyl chloride-functionalized MWNTs (MWNT-COCl). The as-produced MWNT-COCl was immediately reacted without further purification with glycol (50 mL, 0.9 mol) for 48 h at 120 °C. Hydroxyl-functionalized MWNTs (MWNT-OH) (1.5 g) were obtained by repeated filtration and washing.

MWNT-OH (1.0 g) was reacted with 2-bromo-2-methylpropionyl bromide (3.0 g, 13.0 mmol) in $CHCl_3$ (20 mL) in the presence of triethylamine (2.0 mL, 14.3 mmol) and *N*,*N*-dimethylaminopyridine (DMAP, 0.2 g, 1.64 mmol) at 0 °C for 1 h and at room temperature for 48 h. The solid was then separated from the mixture by filtration and washed five times with 200 mL of $CHCl_3$. The raw product was dispersed in 25 mL of $CHCl_3$, filtered, and washed three times to remove any adsorbed 2-bromo-2-methylpropionyl bromide. The black solid was collected and dried overnight under vacuum at 40 °C, affording 0.99 g of MWNT-supported ATRP initiator (MWNT-Br). The synthesis and characterization details are the same as those previously reported by Gao and co-workers.[6,20] TGA measurements showed 23.6% weight loss below 460 °C for MWNT-Br and 15.4% weight loss for MWNT-OH. This 8.2% difference in weight loss corresponds to ~0.55 mmol of initiator groups per gram of MWNT-Br, 0.72 mmol per gram of neat MWNTs, or ~8.6 initiator groups per 1000 carbons.

Scheme 1. Functionalization of Multiwalled Carbon Nanotubes (MWNTs) with Poly(glycerol monomethacrylate) (PolyGMA) by Atom Transfer Radical Polymerization (ATRP), Esterification of the Hydroxyl Groups of MWNT-PolyGMA, and Metal Sequestration/Reduction by the Grafted Polyacid Chains

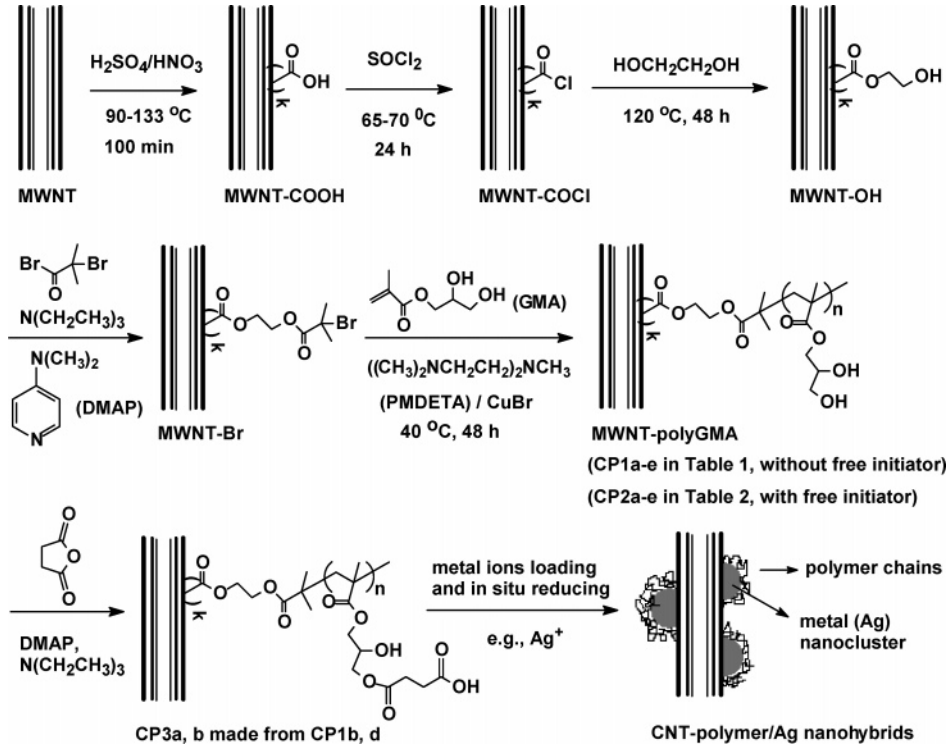

Table 1. Polymerization of Glycerol Monomethacrylate (GMA) Initiated with Multiwalled Carbon Nanotube-Based Macroinitiator (MWNT-Br) without Free Initiator

code	R_{weight}[a]	R_{mole}[b]	$M_{n,theory}$[c]	conv (%)[d]	$M_{n,con}$[e]	f_{wt}%[f]	$M_{n,TGA}$[g]
CP1a	1.0:1	11:1:3:3	1750	65	1140	51	1450
CP1b	1.3:1	15:1:3:3	2400	78	1870	63	2360
CP1c	2.2:1	25:1:3:3	4800	80	3840	75	4170
CP1d	4.4:1	50:1:3:3	8000	73	5840	83	6780
CP1e	8.8:1	100:1:3:3	16000	76	12160	90	12500

[a] The weight ratio of monomer/MWNT-Br. [b] The mole ratio of monomer/initiator point/CuBr/PMDETA. [c] $M_{n,theory} = R_{mole} \times$ GMA molar mass. [d] The conversion of GMA monomer calculated from the yield of product: wt of (MWNT-PGMA-MWNT-Br)/wt of monomer. This conversion is generally smaller than the actual value because of loss of product during washing, filtration, and isolation. [e] The number-average molecular weight calculated from the monomer conversion: $M_{n,con} = M_{n,theory} \times$ conversion. [f] The weight fraction of grafted polyGMA calculated from TGA data. [g] The average molecular weight of the grafted polyGMA calculated from TGA data: $M_{n,TGA} = f_{wt}/[(1 - f_{wt}) \times 0.72 \times 10^{-3}]$; herein, 0.72 represents the concentration of initiating sites per gram of MWNTs (mmol/g).

Synthesis of MWNT-PGMA by ATRP without Free Initiator. In these syntheses, polyGMA-coated MWNTs (MWNT-PGMA) were prepared by atom transfer radical polymerization of GMA initiated only with MWNT-Br in the presence of the Cu(I)Br/PMDETA catalyst. Typically (CP1e, Table 1), MWNT-Br (0.121 g), CuBr (29 mg, 0.2 mmol), PMDETA (35 mg, 0.2 mmol), and methanol (4 mL) were placed in a 25 mL dry flask, which was then sealed with a rubber plug. The flask was evacuated and filled thrice with argon. GMA (1.065 g, 6.65 mmol) was injected into the flask using a syringe. The flask was immersed in a water bath at 40 °C, and its contents were stirred for 48 h. The mixture was subsequently diluted with methanol (10 mL) and thrice vacuum-filtered using a filter paper (Fischer). The resulting solid was redispersed in methanol (10 mL) and precipitated by the addition of acetone (100 mL). After filtration followed by drying overnight under vacuum, polyGMA-grafted MWNT (CP1e, 0.93 g) was obtained.

Polymerization of GMA Initiated with MWNT-Br and Ethyl 2-Bromoisobutyrate. To investigate the growth of polyGMA from the MWNT surface, a soluble initiator (ethyl 2-bromoisobutyrate) was added to the reaction as a co-initiator. The protocol was the same as that described above. Typically (CP2e, Table 2), MWNT-Br (31.0 mg), ethyl 2-bromoisobutyrate (26.6 mg, 0.136 mmol), CuBr (33 mg, 0.229 mmol), PMDETA (40 mg, 0.231 mmol), and methanol (5 mL) were placed in a 25 mL dry flask, which was then sealed with a rubber plug. The flask was evacuated and filled thrice with argon. GMA (1.598 g, 10 mmol) was injected into the flask using a syringe. The flask was immersed in a water bath at 40 °C, and its contents were stirred for 48 h. The mixture was subsequently diluted with methanol (5 mL) and vacuum-filtered using a filter paper (Fischer), to collect both the filtered solid and the filtrate. The filtrate was purified by passing through an alumina column, concentrated under a rotary distiller, and then dried under vacuum. GPC measurement indicated that the number-average molecular weight (M_n) and the polydispersity index (PDI, M_w/M_n) of the collected free polyGMA were 17 000 and 3.75, respectively. The filtered solid was treated by washing, redispersing, and vacuum filtering, as for the preparation of MWNT-PGMA in the absence of any soluble initiator. The resulting solid was redispersed in methanol (10 mL) and precipitated by the addition acetone

Table 2. Polymerization of Glycerol Monomethacrylate (GMA) Initiated with Multiwalled Carbon Nanotube-Based Macroinitiator (MWNT-Br) and Free Initiator (Ethyl 2-Bromoisobutyrate)[a]

code	R_{weight}[b]	R_{mole}[c]	$M_{n,theory}$	f_{wt}%	$M_{n,TGA}$[d]	$M_{n,GPC}$	M_w/M_n	R_{MW}[e]
CP2a	15.9/1/3.8	5.0/1	800	46	720	3000	1.49	3.75
CP2b	20.2/1/1.7	13.5/1	2160	55	1700	3900	1.89	1.81
CP2c	23.5/1/1.33	20.0/1	3200	68	2950	8100	1.97	2.53
CP2d	31.7/1/0.86	40.0/1	6400	80	5550	11300	2.95	1.77
CP2e	51.5/1/0.86	65.0/1	10400	88	10200	17000	3.75	1.63

[a] The mole ratio of total initiating sites/CuBr/PMDETA is 1/1.5/1.5. [b] The weight ratio of monomer/MWNT-Br/ethyl 2-bromoisobutyrate. [c] The mole ratio of monomer to total initiating points. [d] The average molecular weight calculated from TGA results: $M_{n,TGA} = f_{wt}/[(1 - f_{wt}) \times 0.72 \times 10^{-3}]$; $M_{n,TGA}$ for CP2a is the molar mass of neat polyGMA units excluding the weight fraction of organic moieties attached onto MWNT-Br, because of the great influence of such weight fraction on the calculation for such a low R_{mole}. [e] $R_{MW} = M_{n,GPC}/M_{n,theory}$.

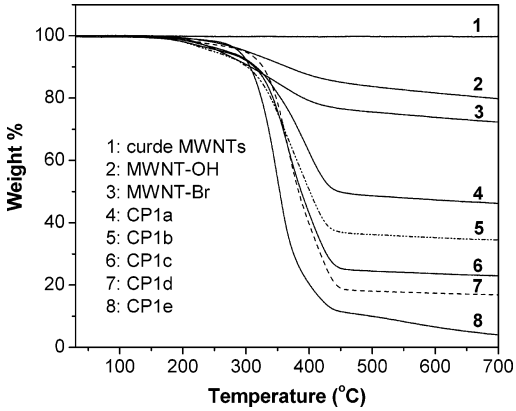

Figure 1. Thermogravimetric analysis (TGA) weight loss curves obtained under nitrogen for pristine multiwalled carbon nanotubes (MWNTs), hydroxyl-functionalized MWNTs (MWNT-OH), MWNT-based macroinitiator (MWNT-Br), and poly(glycerol monomethacrylate)-grafted MWNTs (MWNT-polyGMA) without free initiator (CP1 series).

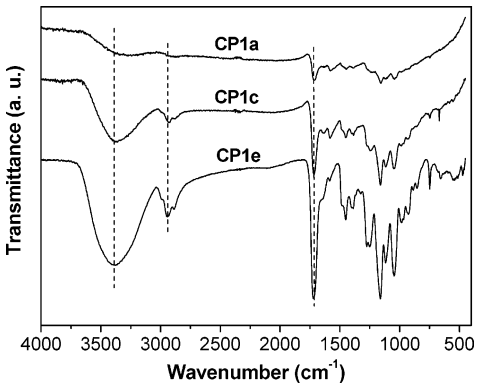

Figure 2. Fourier transform infrared (FTIR) spectra of CP1a (51 wt % polymer), CP1c (75 wt % polymer), and CP1e (90 wt % polymer) samples of poly(glycerol monomethacrylate)-grafted multiwalled carbon nanotubes (MWNT-polyGMA) prepared in the absence of free initiator (CP1 series).

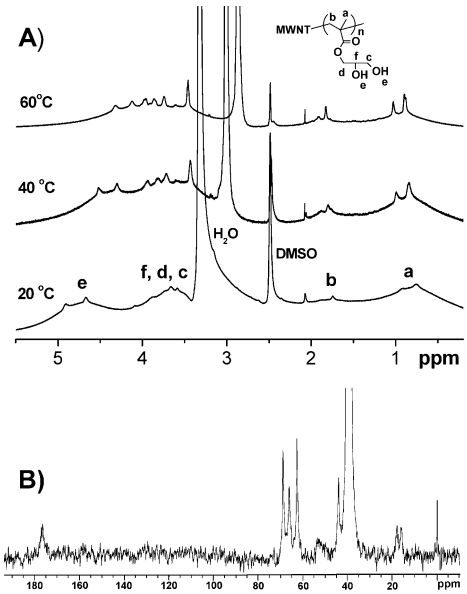

Figure 3. (A) ^{1}H NMR spectra of poly(glycerol monomethacrylate)-grafted multiwalled carbon nanotubes, CP1e (90 wt % polymer), recorded at 20, 40, and 60 °C. (B) ^{13}C NMR spectrum of CP1e recorded at 20 °C.

(100 mL), giving 0.12 g of product after filtration and drying overnight under vacuum. TGA measurement demonstrated that the grafted polymer content was around 88% by mass.

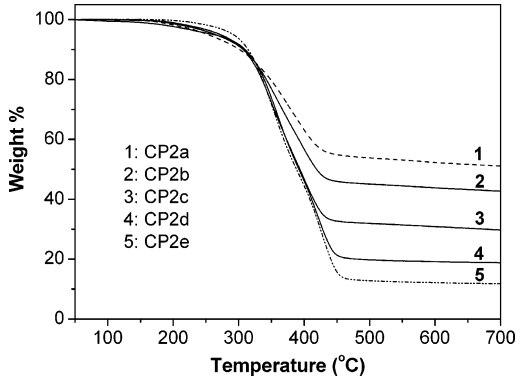

Figure 4. Thermogravimetric analysis (TGA) weight loss curves obtained under nitrogen for poly(glycerol monomethacrylate)-grafted multiwalled carbon nanotubes (MWNT-polyGMA) prepared using MWNT-based macroinitiator (MWNT-Br) and ethyl 2-bromoisobutyrate as co-initiators (CP2 series).

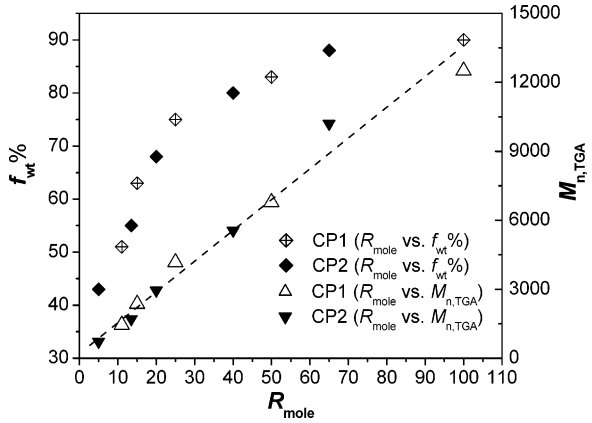

Figure 5. Weight fraction of grafted poly(glycerol monomethacrylate) (polyGMA) calculated from the thermogravimetric analysis (TGA) data (f_{wt}%) and the average molecular weight of the polyGMA calculated from TGA ($M_{n,TGA}$) as a function of molar feed ratio (R_{mole}) for the carbon nanotube surface-initiated polymerizations in the presence and absence of free initiator.

Derivatization of MWNT-PGMA To Synthesize Multicarboxyl Polymer-Coated MWNTs (CP3). The hydroxyl groups of polyGMA can be partially converted to carboxylic acid groups by reaction of MWNT-PGMA with succinic anhydride in the presence of triethylamine and DMAP.[35] CP1b and CP1d were further modified by this method in our experiments. Typically, CP1d (0.3 g), succinic anhydride (0.5 g, 5 mmol), triethylamine (1 mL, 7.17 mmol), DMAP (0.1 g, 0.82 mmol), and DMF (35 mL) were added to a 100 mL flask immersed in an ice−water bath. The reaction temperature was gradually increased to 40 °C and maintained for 24 h with continual stirring. The reaction mixture was separated by four centrifugation cycles (ca. 2−3 h per cycle at a rate of 6000 rpm). The collected solid was redispersed in DMF (10 mL) and precipitated by addition of acetone (100 mL). After filtering and vacuum-drying, 0.43 g of black solid powder (CP3b) was obtained. The derivatized product of CP1b was designated as CP3a.

Preparation of CP3/Metal Hybrid Nanocomposites Templated from CP3. The high density of carboxylic acid groups in CP3 can be used to chelate metal ions, giving rise to CP3/metal nanocomposites or nanowires. The synthesis of a silver nanocomposite is used as an example to illustrate the process. Typically, CP3b (150 mg), NaOH aqueous solution (10 mL, 1 M), and water (50 mL) were placed in a 250 mL flask. The mixture was sonicated for 3 min, stirred at room temperature for 2 h, and then separated by centrifugation (ca. 2−3 h per cycle at a rate of 6000 rpm with a 50 mL plastic centrifuging tube) until the pH of the aqueous phase approached 7.0 (at least four cycles with ca. 40 mL of added water

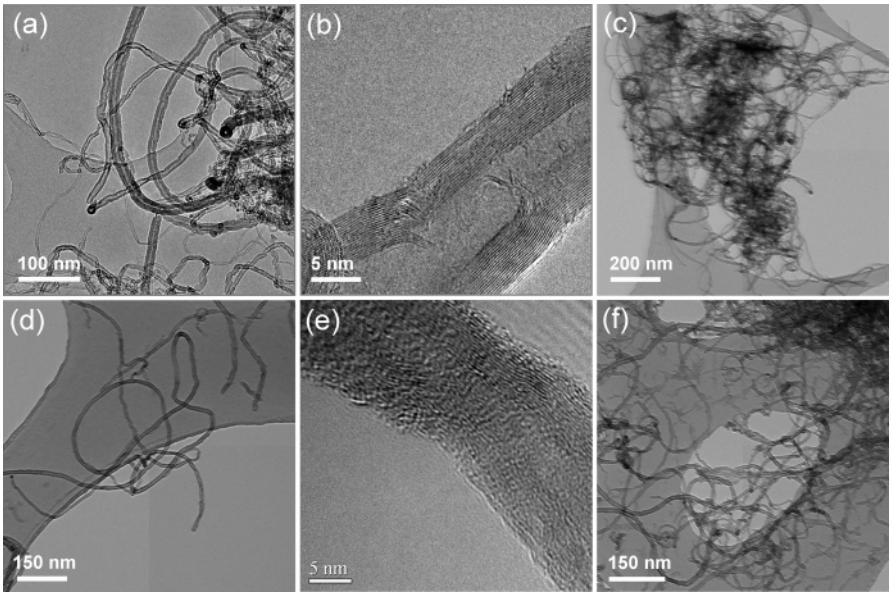

Figure 6. Transmission electron microscopy (TEM) images of pristine multiwalled carbon nanotubes (MWNTs) (a, b) and MWNTs oxidized for 100 min (c, d, e) and for 3.5 h (f).

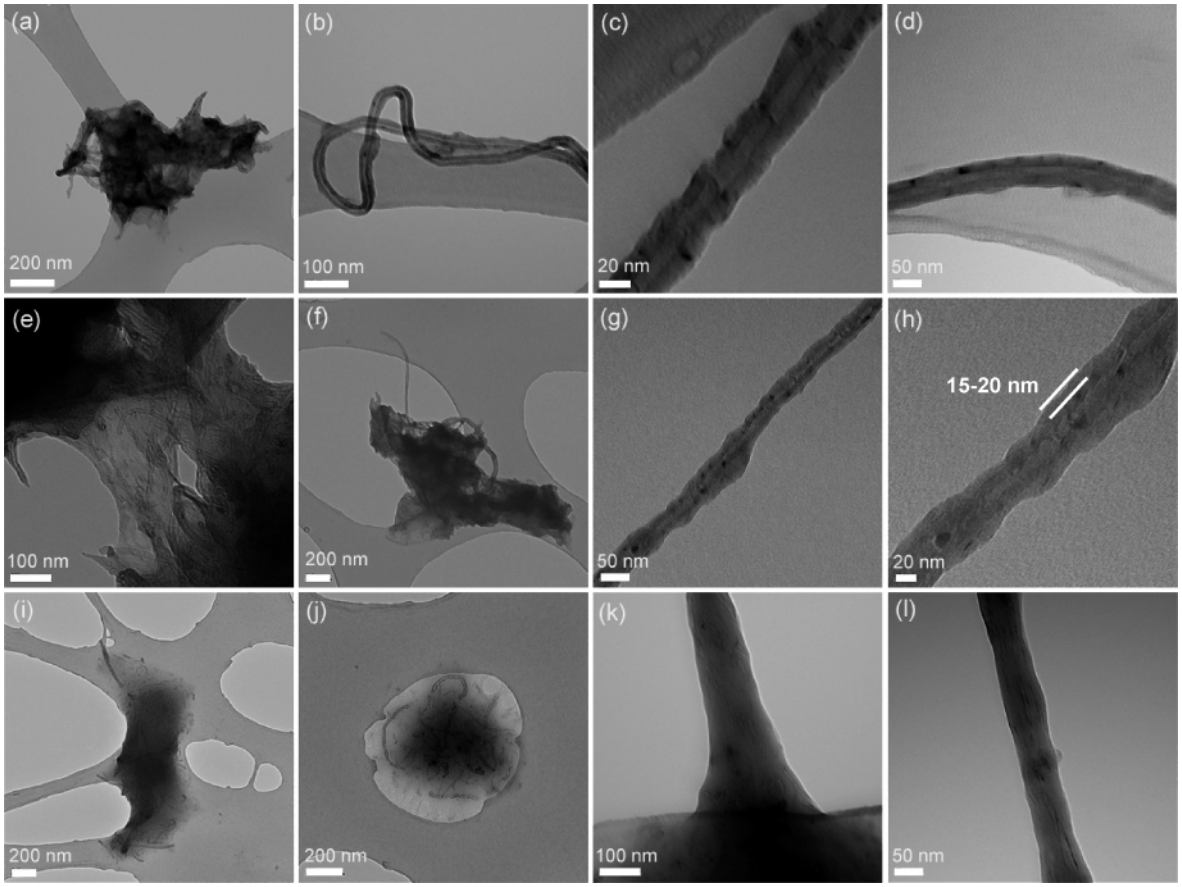

Figure 7. Transmission electron microscopy (TEM) images obtained for samples of poly(glycerol monomethacrylate)-grafted MWNTs (MWNT-polyGMA) without free initiator (CP1 series): (a−d) CP1b (63 wt % polyGMA), (e−h) CP1d (83 wt % polyGMA), and (i−l) CP1e (90 wt % polyGMA).

per cycle was required). The separated solid was redispersed in water (100 mL) with the aid of an ultrasonics bath for ca. 3 min. The solution (15 mL) was then transferred into a 50 mL flat-bottomed flask equipped with a magnetic bar, and the $AgNO_3$ aqueous solution (10 mL, 0.01 M) was added dropwise to the flask with vigorous stirring. The mixture was stirred at room temperature for 2 h and separated by four centrifugation cycles (ca. 2−3 h per cycle at a rate of 6000 rpm with a 50 mL plastic centrifuging tube). In each case ~35 mL of water was added to the plastic centrifuge tube to aid dispersion of the collected solid.

Results and Discussion

I. Synthesis of MWNT-PGMA. General Description. It was reported that the ATRP of GMA is fast and well-controlled in polar solvents such as methanol even

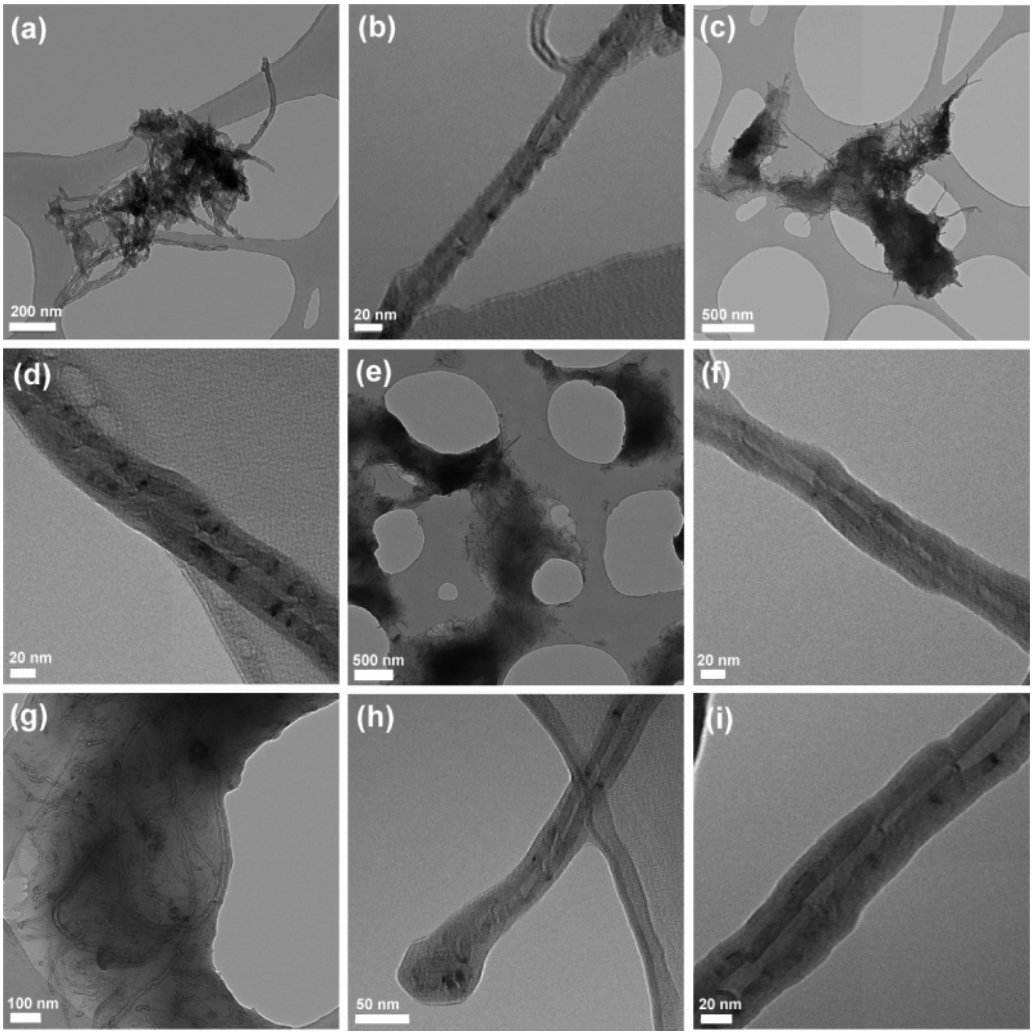

Figure 8. Transmission electron microscopy (TEM) images obtained for samples of poly(glycerol monomethacrylate)-grafted multiwalled carbon nanotubes (MWNT-polyGMA) prepared with MWNT-based macroinitiator (MWNT-Br) and ethyl 2-bromoisobutyrate (CP2 series) as co-initiators: (a, b) CP2a (46 wt % polyGMA), (c, d) CP2c (68 wt % polyGMA), (e, f) CP2d (80 wt % polyGMA), and (g−i) CP2e (88 wt % polyGMA).

at relatively low temperatures.[34] Thus, our ATRP syntheses of MWNT-PGMA were conducted in methanol at around 40 °C. The overall synthesis route is illustrated in Scheme 1.

Well-defined, functionalized nanosurfaces and nanomaterials are crucial in the exploration, fabrication, processing, modification, and amelioration of materials and devices. According to Gao and co-workers, the amount of grafted polymer on MWNT surfaces can be controlled by the feed ratio of monomer to MWNT-Br (R_{feed}) for a wide range of vinyl monomers, including styrenics (e.g., styrene and sodium 4-styrenesulfonate),[20,24] (meth)acrylates (e.g., methyl methacrylate and *tert*-butyl methacrylate),[6,26] and acrylamides (e.g., *N*-isopropylacrylamide).[27] In this paper, we also studied several polymerizations with different R_{feed}. The reaction conditions and selected results are summarized in Table 1. Characterization data will be described in the following paragraphs. The extent of grafted polyGMA also can be efficiently controlled by adjusting the R_{feed} over a wide range (at least 51−90 wt %), despite the GMA monomer containing two hydroxyl groups. This excellent tolerance of functionality demonstrates that ATRP is a powerful and versatile tool in the design and synthesis of hydrophilic polymer-related materials and polymer brushes, since it is relatively difficult to grow functional polymers from solid substrates directly from functional monomers by cationic or anionic polymerization.[34,36]

TGA Measurement. The TGA weight loss curves of the resulting nanohybrids are displayed in Figure 1. Weight loss curves of pristine MWNTs, MWNT-OH, and MWNT-Br are also shown as a comparison in Figure 1. The weight loss of pristine MWNTs below 700 °C is less than 3%. There is an obvious weight loss stage between 200 and 460 °C for MWNT-OH (15.4%) and MWNT-Br (23.6%). The initiating group density of MWNT-Br, estimated from its 8.2% weight loss, is ca. 0.55 mmol per gram of MWNT-Br, 0.72 mmol per gram of neat MWNTs, or ca. 8.6 initiator groups per 1000 carbons. This value is similar to an earlier study by Gao and co-workers[6] (0.448 mmol per gram of MWNT-Br), whereas it is 2-fold higher than that of SWNT-Br[25] (4.3 initiator functions per 1000 carbon atoms). Such a high density of initiator groups implies that (1) the MWNTs contain much more defects than the SWNTs, (2) the CVD tube surfaces have abundant defects distributed not only on the ends but also over the whole convex body, (3) the tubes can become enwrapped in the grafted polymer chains to produce single-molecule nanowires or nanocables with conductive cores and insulating shells, and (4) such a high density of initiator sites may produce

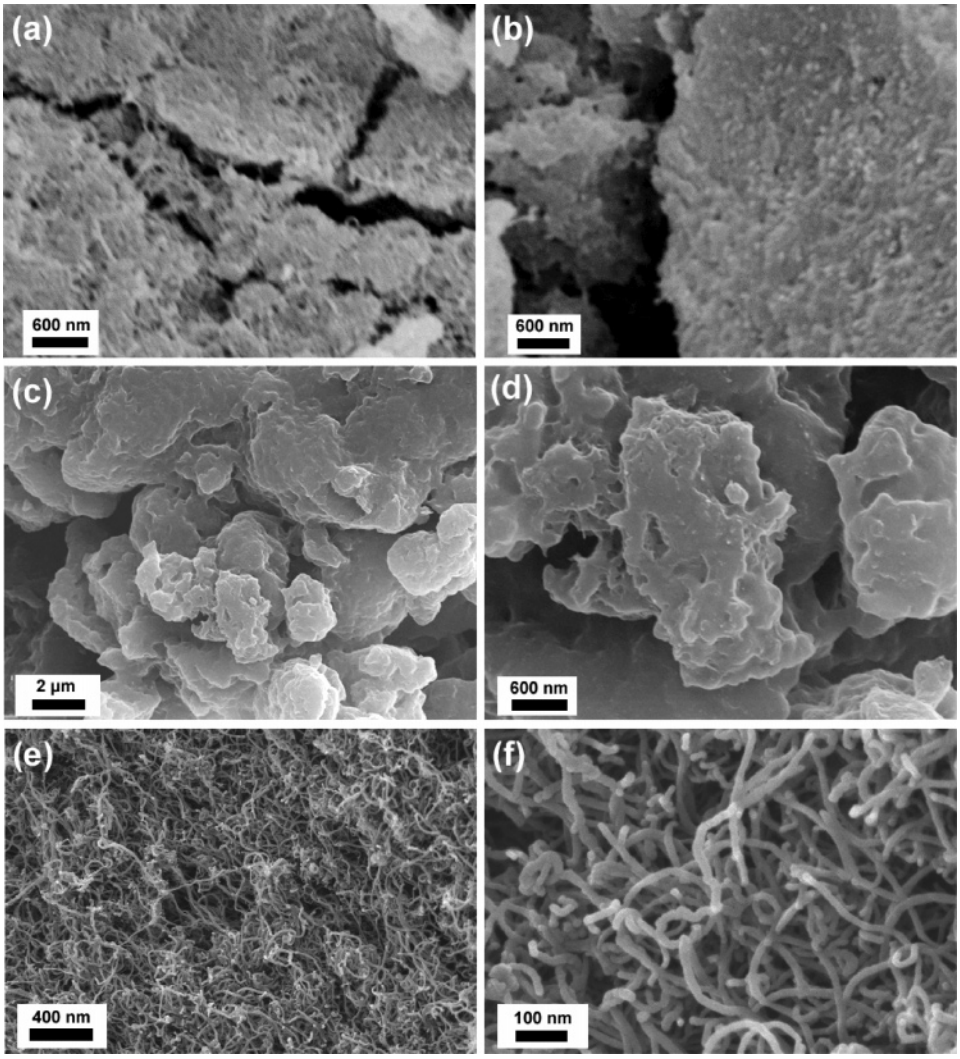

Figure 9. Representative scanning electron microscopy (SEM) images obtained for samples of poly(glycerol monomethacrylate)-grafted MWNTs (MWNT-polyGMA) prepared in the absence of free initiator (CP1 series): (a) CP1b (63 wt % polyGMA), (b) CP1c (75 wt % polyGMA), (c, d) CP1e (90 wt % polyGMA), and (e, f) pristine MWNTs.

higher polydispersities for the grafted polymer due to the increased probability of termination between neighboring growing chains.

In addition, the weight loss of MWNT-polyGMA samples can also be easily calculated from Figure 1. The corresponding data are summarized in Table 1, with greater weight losses being observed as the monomer/MWNT-Br feed ratio is increased. The number-average molecular weight calculated from the TGA results ($M_{n,TGA}$) increased linearly from 1450 to 12 500 as the monomer/initiator molar feed ratio varied from 11 to 100. The number-average molecular weights calculated from the monomer conversion ($M_{n,con}$) are a little lower than the corresponding $M_{n,TGA}$ values due to losses incurred during purification but also increased linearly from 1140 to 12 160 (see Table 1).

FTIR and NMR Spectra. The chemical structure of the MWNT-PGMA hybrid nanowires was confirmed by FTIR and NMR spectroscopy studies. The representative FTIR spectra are displayed in Figure 2. After polyGMA was grown on the tube surfaces, the characteristic absorption peaks assigned to carbonyl (C═O), ethylene (−CH_2−), and hydroxyl (−OH) vibrations were clearly visible at 1722, 2980, and 3450 cm^{-1}, respectively, and the peak intensity increases considerably with increasing levels of grafted polymer.

The polyGMA-functionalized MWNTs showed good solubility/dispersibility in polar solvents such as methanol, ethanol, DMSO, and DMF. Figure 3 shows the typical ^1H and ^{13}C NMR spectra of the nanohybrids in DMSO-d_6. In the ^1H NMR spectrum (Figure 3A), the proton signals due to CH_3−, −CH_2−, −CH_2O−/−CHO−, and OH− are found at δ 0.8, 1.8, 3.4−4.2, and 4.3−5.3 ppm, respectively, at 20 °C. Increasing the solution temperature led to the upfield shift of active hydrogen peaks (e.g., −OH and H_2O). Hence, the two peaks at 4.65 and 4.9 ppm were assigned to the two hydroxyl groups in polyGMA. In addition, these two peaks disappeared after the addition of D_2O in the measuring sample, which further confirmed the assignment. For the samples coated with high levels of grafted polymer (e.g., CP1d and CP1e), ^{13}C NMR spectrua can be obtained due to their greater solubility. A representative ^{13}C NMR spectrum is shown in Figure 3B. The carbon signals of the polyGMA moieties are assigned as follows: 177 (CO), 70−60 (CHO and CH_2O), 44 (C), 18 (CH_2), and 16 ppm (CH_3).

Polymerization in the Presence of Free Initiator and the Estimation of Molecular Weight. Generally, two methods can be used to estimate the molecular weight of surface-initiated polymers grafted onto a solid surface: (i) chain cleavage from the surface followed by

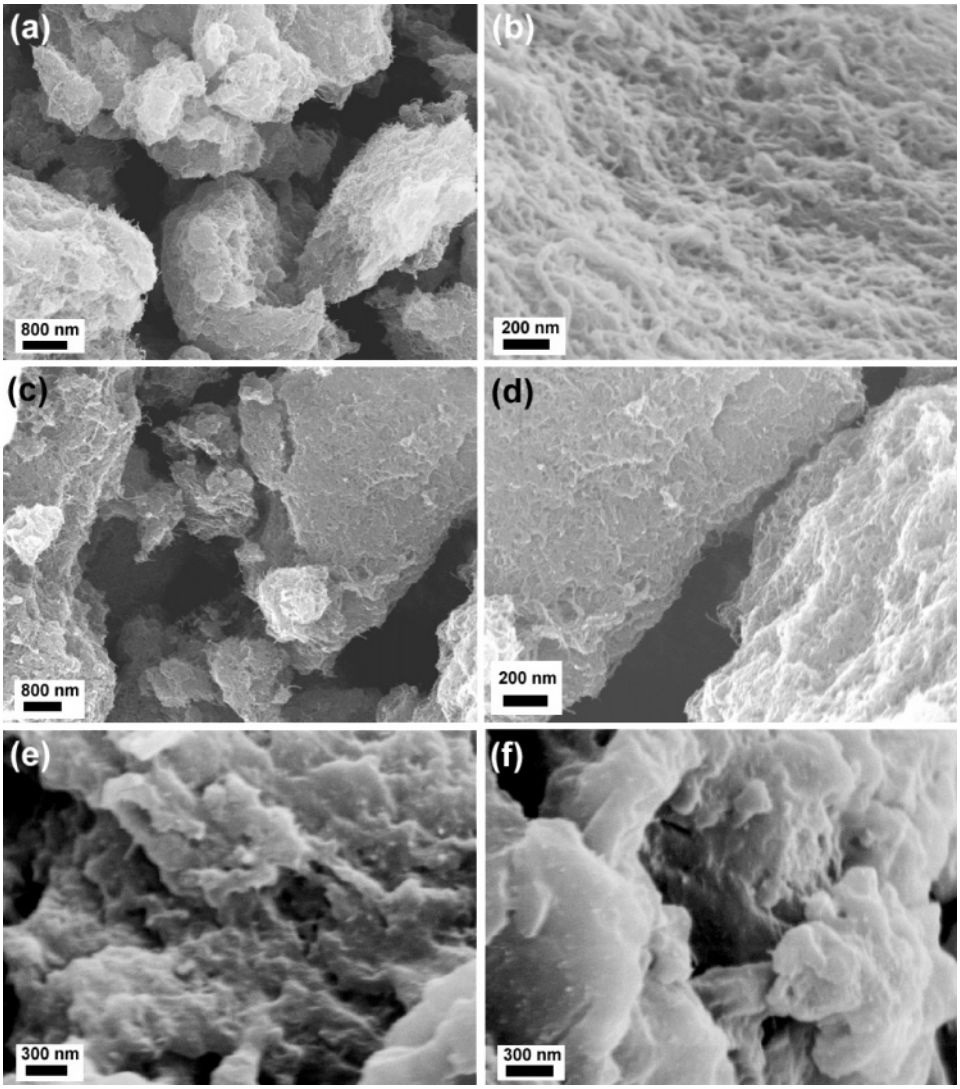

Figure 10. Representative scanning electron microscopy (SEM) images obtained for samples of poly(glycerol monomethacrylate)-grafted multiwalled carbon nanotubes (MWNT-polyGMA) prepared with MWNT-based macroinitiator (MWNT-Br) and ethyl 2-bromoisobutyrate (CP2 series) as co-initiators: (a, b) CP2a (46 wt % polyGMA), (c, d) CP2c (68 wt % polyGMA), (e) CP2d (80 wt % polyGMA), and (f) CP2e (88 wt % polyGMA).

SEC analysis and (ii) addition of free initiator followed by SEC analysis of the soluble polymer. For polymers that are stable in the presence of acid or base, cleavage should not result in any significant changes in the molecular weight distribution.[20,27,31] For less robust polymers such as poly(meth)acrylates, the molecular weight can be estimated by addition of soluble initiator, assuming identical polymerization efficiencies for the substrate-grafted and free initiator. Although the second method has proven effective for certain surface-initiated polymerizations,[37] studies of CNT-supported polymerizations have drawn conflicting conclusions. Adronov et al.[23] reported that, in their hands, SWNT-supported ATRP was not well-controlled in terms of both the target molecular weight and polydispersity even when free initiator was added to the reaction solution. However, excellent control was reported by Ford and co-workers in their SWNT-supported ATRP experiments in the presence of soluble free initiator.[25] Interestingly, Gao[6,20,27] and Baskaran et al.[21] reported that the molecular weight can be controlled during surface ATRP from multiwalled tubes as it increases with increasing the feed ratio of monomer/MWNT-Br, but polydispersities are broader than those typically found for homogeneous ATRP syntheses, especially for higher target molecular weights. This implies that (1) MWNTs and SWNTs behave very differently even though they have important similarities and (2) the polymerization on the CNT surfaces is quite complex and differs from the conventional solution or solid-surface polymerizations to some extent.

In this work GMA polymerizations were conducted in both the presence and absence of soluble initiator (see Scheme 1). The reaction conditions and results are summarized in Table 2. Again, the level of grafted polymer on the tube surface was calculated from the corresponding TGA weight loss curve (see Figure 4). The grafted polymer content increased monotonically from 46 to 88% as the monomer/initiator feed ratio was increased from 5 to 65, which is very similar to the case of no free initiator mentioned previously. At the same time, the $M_{n,TGA}$ also increased linearly from 720 to 10 200. This confirms that (1) surface polymerization still occurs in the presence of soluble initiator and (2) the polymer content or number-average molecular weight of the grafted macromolecules can be readily adjusted within a wide range (f_{wt}%: 46 to 88%; $M_{n,TGA}$: ca. 720−10 200) by varying the monomer/co-initiator feed ratio. Like the $M_{n,TGA}$ of CP1, $M_{n,TGA}$ of CP2 is also smaller than the corresponding $M_{n,theory}$, which can be partly attributed

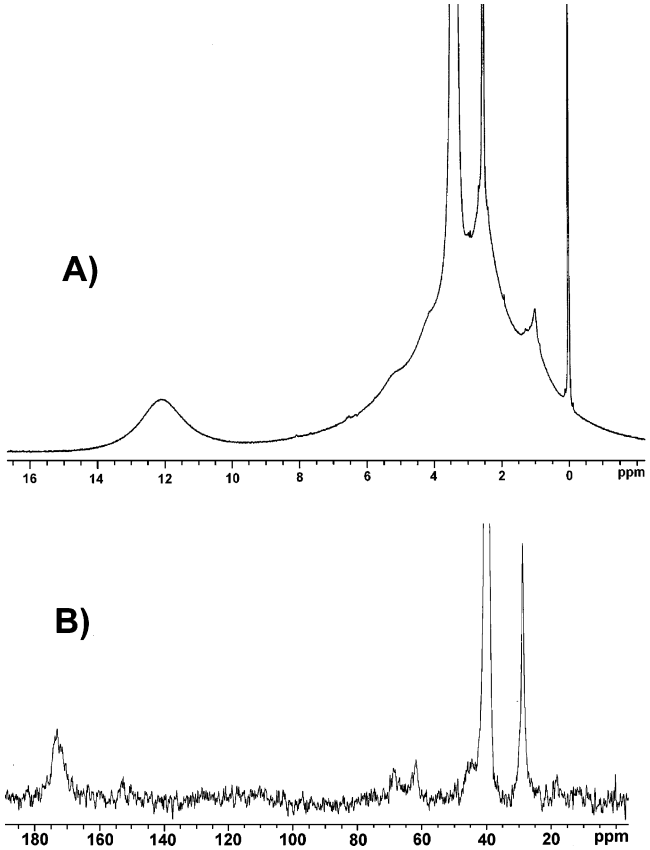

Figure 11. ^{1}H NMR (A) and ^{13}C NMR (B) spectra recorded for sample CP3b prepared by esterification of poly(glycerol monomethacrylate)-grafted multiwalled carbon nanotubes (CP1d) with succinic anhydride.

to (1) incomplete monomer conversion and (2) imperfect initiation efficiency for the grafted initiator sites.

The $M_{n,GPC}$ values of the soluble polymer chains also increase from 3000 to 17 000, while the polydispersities become broader at higher feed ratios. Similar results were previously reported for MWNT-surface initiated polymerization: the amount of grafted polymer can be selected with some certainty, but the polydispersities can be as high as 3−4, especially for higher target degrees of polymerization.[20,21] The high polydispersities for the grafted polymers most likely arise due to the increased probability of termination caused by the relatively high density of anchored initiator sites.[20] The high polydispersities of the free polymers were seemingly caused by the addition of MWNT-Br, since the ATRP of GMA can be relatively well controlled (PDI < 1.5) in methanol in the absence of MWNT-Br.[32] However, the precise mechanistic details are not yet clear. Two further points are noteworthy: (1) $M_{n,GPC}$ is systematically higher than the corresponding $M_{n,theory}$, and (2) the higher the feed ratio (R_{mole}), the lower the $M_{n,GPC}/M_{n,theory}$ ratio. This unusual observation for $M_{n,GPC}$ of the free polymer is possibly due to quenching of the initiating radicals by the carbon nanotubes.[9,29] If this is correct, higher monomer concentrations should lead to lower degrees of quenching because of increased competition between initiation and quenching. Hence, $M_{n,GPC}/M_{n,theory}$ should become smaller. The presence of free initiator has almost no influence on the CNT-initiated polymerization, but the presence of CNTs influences the solution polymerization to some extent.

To confirm that the CNT surface-initiated polymerization in the absence of free initiator is comparable to that conducted in the presence of the co-initiated solution polymerization, the polymer weight loss (f_{wt}%) and $M_{n,TGA}$ as a function of feed ratio for the two cases are displayed in Figure 5. The relationship between R_{mole} and f_{wt}% is similar for the two cases. $M_{n,TGA}$ increases linearly with increasing R_{mole}, and the corresponding R_{mole} vs $M_{n,TGA}$ data lie on a straight line. This confirms that the free initiator has no significant effect on the CNT surface polymerization.

In addition, the ratios of the highest $M_{n,TGA}$ to the lowest value ($M_{n,TGA,highest}/M_{n,TGA,lowest}$) are ~8.6 for the CP1 series and ca. 14 for the CP2 series, respectively, which is in accordance with the corresponding biggest feed ratio to the smallest one ($R_{mole,biggest}/R_{mole,smallest}$ is ca. 8.8 for CP1 series and 13 for CP2, respectively). This provides further evidence for a reasonable degree of control over the amount of grafted polymer obtained in the MWNT surface-initiated polymerizations, whether in the absence or presence of a soluble initiator. Considering the above discussions and the previous reports on CNT-surface ATRP polymerizations, we can conclude that the nanotube itself has a strong effect on these ATRP syntheses.

TEM Observations. The morphological structures of pristine, oxidized, and polyGMA-grafted MWNTs were examined by TEM. Figure 6 shows TEM images of the pristine MWNTs and also the MWNT-COOH. The pristine tube surface is featureless, and there are little or no traces of amorphous carbon (see Figure 6a,b). After oxidation by H_2SO_4/HNO_3 for 100 min, most of the tubes retain their tubular structure with mean lengths of the order of micrometers, but some tubes and certain tube sections were heavily eroded, generating many defects and holes (see Figure 6c−e). Thus, oxidation not only occurred at the outermost wall but also on the inner walls, providing more reactive sites than predicted. After oxidation for longer times (3−4 h), the tubes were truncated, and many tubes disintegrated (see Figure 6f). Hence, controlling the reaction time is essential in order to obtain well-defined oxidized tubes (MWNT-COOH) under these conditions.

Figure 7 depicts representative TEM images for the CP1 series of samples using 100 min-oxidized MWNTs as raw material. For CP1b (63 wt % polyGMA), polymer-coated tubes are clearly produced (Figure 7a). The polymer shell surrounding an individual nanowire is very uniform (Figure 7b). Under higher magnification, the tube is clearly enwrapped by several nanometers of polymer chains, although the precise boundary between the tube and the polymer layer is somewhat indistinct (Figure 7c,d). For high levels of grafting, the outer layer of polymer becomes the continuous phase and free-standing films are obtained. The products resemble tube-embedded nanocomposites with a similar structure to that of steel-fiber reinforced concrete (Figure 7e,f,i j). Under higher magnification, "core−shell" structures are evident for CP1d with a shell thickness of 15−20 nm (Figure 7g,h). For CP1e, the nanowires tend to self-assemble, forming aggregates in which some tubes become aligned by the interaction between the polymer chains (Figure 7k,l). The TEM observations are consistent with the TGA results: the grafted polymer contents can be efficiently controlled by adjusting the feed ratio. It is noteworthy that the electron beam may destroy polymer chains and possibly even the tubes themselves, especially at high resolution. Thus, the amount of polymer observed in the presented TEM images probably represents a lower limit.

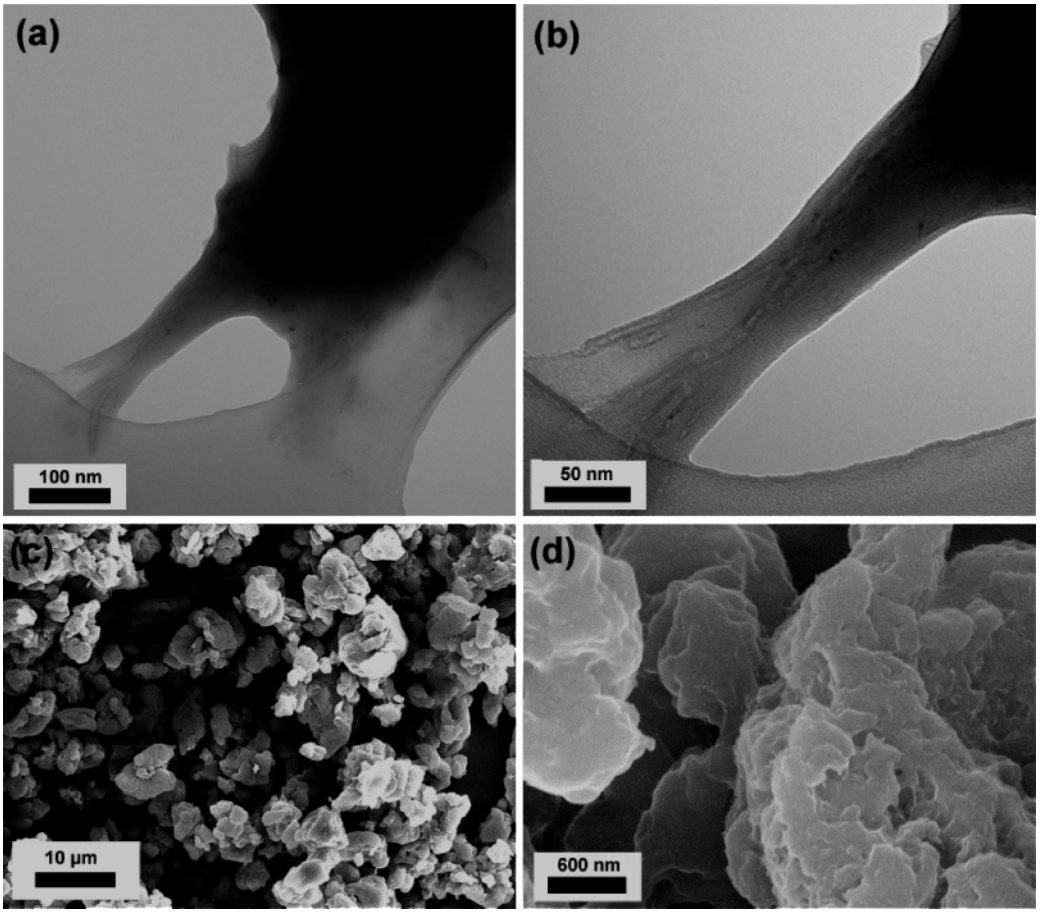

Figure 12. Transmission electron microscopy (TEM) images (a, b) and scanning electron microscopy (SEM) images (c, d) recorded for sample CP3b, which was prepared by esterification of poly(glycerol monomethacrylate)-grafted multiwalled carbon nanotubes (CP1d) with succinic anhydride.

To confirm that the surface polymerization has comparable efficiency when conducted in the presence or absence of free initiator, the CP2 series of samples were also characterized by TEM (see Figure 8). For CP2a, the tubes are well-separated even at a relatively low polymer grafting density (Figure 8a). Under higher magnification, the tube surface looks hairy due to the growth of polymer chains on the tube (Figure 8b). For CP2c and CP2d, the polymer−nanotube hybrids were observed under lower magnification to illustrate the uniformity of the polymer grafting (Figure 8c,e). For the individual tubes or separated tube sections, polymer layers of 8−15 nm thickness were evident due to the differing electron contrast of the polyGMA with the MWNTs (see Figure 8d,f). Furthermore, these polymer overlayers appear to be very smooth and even, suggesting high grafting densities are achieved. For CP2e, a nanotube-embedded polymer composite similar to that found for CP1e was observed (see Figure 8g), indicating an extremely high degree of grafting. A core−shell structure was also evident for the separated nanotubes (Figure 8h,i). These TEM observations further demonstrate that the grafted polymer density for the CP2 series can be efficiently controlled by adjusting the feed ratio despite the presence of soluble initiator and the coating integrity is equivalent to that achieved in the absence of soluble initiator.

SEM Observations. Figure 9 displays the SEM images of samples from the CP1 series. For CP1b, a rodlike morphology was observed due to the relatively low degree of grafting (Figure 9a). When the degree of grafting was increased, rodlike structures were observed protruding through the polymer overlayer (see Figure 9b). For CP1e, only the bulk polymer phase was observed due to the high polymer grafting density (Figure 9c,d). As a comparison, SEM images of nongrafted tubes are also shown (Figure 9e,f), exhibiting clearly distinctive tubelike morphology.

The CP2 series of samples were also studied by SEM (see Figure 10). Similarly, rodlike structures are observed in samples with lower grafting densities (CP2a, see Figure 10a,b), while evidence for coated polymer brushes can be discerned from the reduced spacing between the nanotubes. The rods become less distinct at higher grafting densities (see Figure 10c−e) with eventually only a compact mass being observed (Figure 10f). These SEM observations agree with TEM and other measurements: the morphology changes from core−shell nanowires to nanotube-embedded polymer nanocomposites as the polymer grafting density is increased.

II. Derivatization of MWNT-PGMA. The high density of hydroxyl groups on the grafted polyGMA allows the design of functional hybrid nanomaterials based on polymer-coated CNTs. In this study we have converted the hydroxyl groups into carboxylic acids by esterification chemistry (see Scheme 1). MWNT-polyGMA was reacted with excess succinic anhydride in the presence of a basic catalyst (e.g., triethylamine and DMAP), affording samples with high densities of carboxylic acids (CP3 series). Samples of CP3a and CP3b were prepared using CP1b and CP1d as reactive ma-

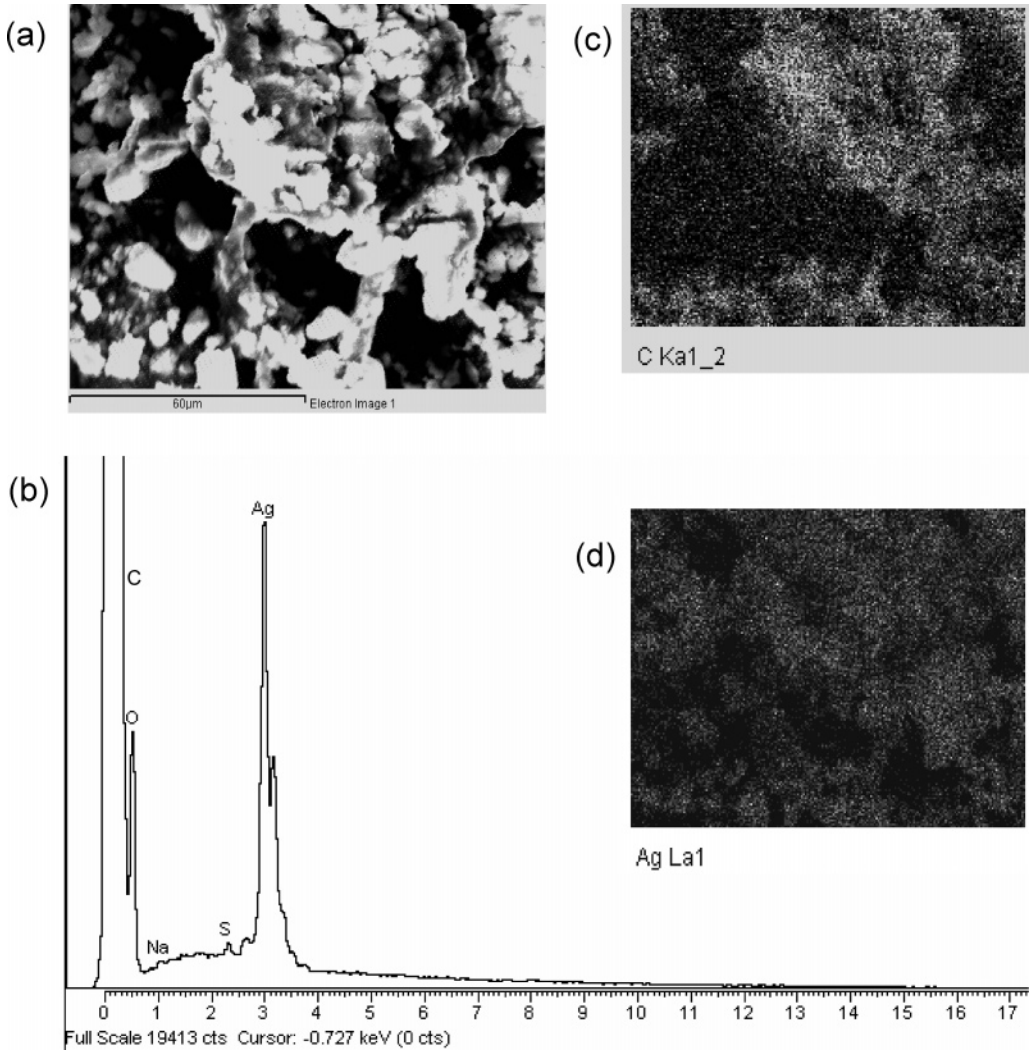

Figure 13. Scanning electron microscopy (SEM) and energy dispersive spectroscopy (EDS) analysis of CP3b prepared by esterification of poly(glycerol monomethacrylate)-grafted multiwalled carbon nanotubes (CP1d) with succinic anhydride: (a) SEM image of EDS analysis area, (b) EDS spectrum, (c) carbon elemental mapping, and (d) silver elemental mapping.

terials, respectively. The degrees of esterification for CP1b and CP1d are approximately 52 and 57% (100% esterification corresponds to two succinic acid units per methacrylate unit), respectively, according to TGA analyses (curves not shown).

The measurements of FTIR and NMR confirmed that esterification had occurred, as expected. The carbonyl absorption band shifted from 1722 to 1734 cm^{-1} (spectrum is not shown). The hydroxyl absorption band intensity at 3380 cm^{-1} also strongly decreased after esterification. In the ^1H NMR spectrum of CP3b (Figure 11A), the hydroxyl signals of polyGMA at δ 4−5 ppm were significantly attenuated, and a new signal appeared at 12 ppm that was assigned to the −COO***H*** signal. In the quantitative ^{13}C NMR spectrum recorded for CP3b (Figure 11B), the methylene signals at δ 28 ppm and carbonyl signals at 174 ppm increased strongly compared to those of CP1d, confirming the presence of succinic acid residues.

The structure and morphology of the esterified MWNTs were studied by TEM and SEM. Figure 12 displays representative images for CP3b. Like CP1e, the nanotubes of CP3b were completely obscured by the surface-grafted polymer chains. These composites form a free-standing film on the TEM grid. There is some evidence for self-assembled fiberlike aggregates comprising aligned nanotubes (Figure 12b). In the SEM images of CP3b, the tubelike morphology was difficult to verify due to the relatively thick grafted polymer overlayer (Figure 12c,d).

III. Metal Loading. The esterified MWNTs contain a relatively high density of carboxylic groups, which can be used to sequester metal ions and hence to prepare CNT-reinforced metal−polymer nanocomposites (higher grafted polymer densities) or nanorods (lower grafted polymer densities).

Using amphiphilic copolymer-based cylinders as templates, Schmidt[38] and Müller et al.[39] prepared gold, magnetic, and semiconducting nanowires, which opened up new possibilities for the fabrication of novel organic−inorganic/metal hybrid nanowires or nanorods. On the other hand, oxidized CNTs can also be used as scaffolds to adsorb metal ions (e.g., Ag^+, Pd^{2+}, Cu^{2+}, and Cd^{2+}),[40,41] metal colloids, nanoparticles, or rare earth oxides,[42] affording hybrid nanomaterials or nanodevices. Metals such as Ti, Ni, Pd, Au, Al, and Fe can also be coated onto CNT surfaces by electron-beam evaporation.[43] In this study, CP3 was used to sequester metal ions in order to prepare MWNT-reinforced metal−polymer nanocomposites. This novel template combines the features of CNTs and polymer cylinders. Compared with the use of pristine or oxidized CNTs as templates, our

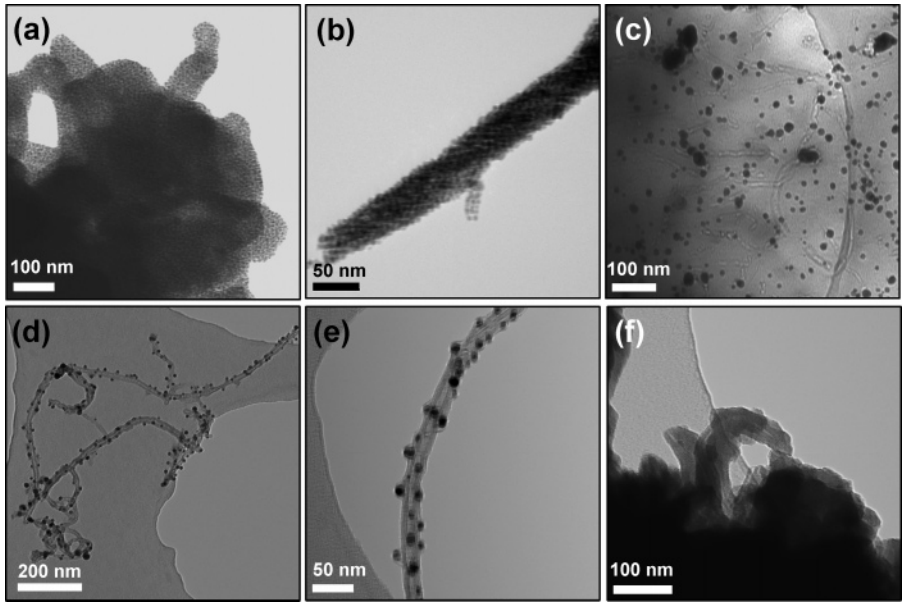

Figure 14. Transmission electron microscopy (TEM) images of functionalized multiwalled carbon nanotubes (MWNTs)/metal (ion) nanocomposites: (a, b) CP3b/Ag with a silver concentration of ca. 0.46 g per gram of CP3b, (c) CP3b/Ag with a silver concentration of ca. 0.15 g per gram of CP3b, (d) CP3a/Ag hybrid nanowire, (e) poly(acrylic acid)-grafted MWNTs (MWNT-PAA)/Ag nanowire section, and (f) CP3/La^{3+} nanocomposites.

strategy offers three advantages: (1) the metal ion loading can be controlled by the grafted polymer density, (2) the metal-loaded MWNTs are relatively stable due to the protective nature of the polymer overlayer, and (3) hybrid polymer/metal nanocomposites can be readily obtained.

After sequestration of metal ions by CP3, two possible outcomes might be expected: (1) if the metal ions are evenly dispersed within the cylindrical polymer shell, core−shell hybrid nanowires or nanocomposites should be obtained; (2) if the sequestered metal ions are locally aggregated, necklace-like nanostructures should be obtained. CP3 was successfully loaded with Ag^+, Co^{2+}, Ni^{2+}, Au^{3+}, Y^{3+}, and La^{3+} ions. As a typical example, we will focus the synthesis and characterization of the resulting CP3/Ag nanocomposites in this paper.

For a given polyacid-grafted MWNT, the silver loading can be easily controlled by varying the molar feed ratio of metal ions to the template. The loading capacity is ca. 0.46 g of silver per gram of CP3b, corresponding to ca. 4.6 g of silver per gram of carbon tubes, as confirmed by TGA measurements. Using nonfunctionalized nanotubes as the reference, the metal ion capacity of CP3 is higher than that of pristine or oxidized CNTs by 1−2 orders of magnitude.[40] Furthermore, it may be possible to improve this capacity further by optimizing reaction conditions such as pH, concentration, and reaction time. Because of its lower grafted polymer density, the metal ion capacity of CP3a is ∼50% that of CP3b. Therefore, the loading capacity can be significantly increased by increasing the grafted polymer content.

Preliminary morphological observations and elemental analyses for these metal ion-loaded nanocomposites were conducted using an SEM instrument equipped with an EDS analyzer. As shown in Figure 13a, the morphology of CP3/Ag is very similar to that of its CP3 precursor. Because of the high polymer loading, the morphology of the underlying nanotubes is rarely observed. EDS analysis confirmed a high silver concentration as expected, as well as carbon, oxygen, and small amounts of sulfur and sodium (Figure 13b). The relatively weak sodium signal indicated that most of the Na^+ ions associated with the modified CP3 were exchanged with Ag^+. Further elemental mapping analysis confirmed that the distribution of silver was relatively uniform and is in accordance with the SEM morphology (Figure 13d).

TEM was also used to characterize the resulting nanocomposites (see Figure 14). Interestingly, nanobeads or nanoclusters, dispersed evenly within the CP3 matrix, were observed for the CP3/Ag sample. At higher Ag^+/CP3 feed ratios, a greater concentration of silver nanobeads of ca. 3−5 nm diameter were found (Figure 14a,b). At lower feed ratios, fewer silver nanoparticles are formed. These are distributed within the composites and have an average diameter of ca. 10 nm (Figure 14c). At lower grafted polymer densities, silver nanoparticle-decorated nanowires were obtained (Figure 14d).

The observed silver aggregates are unusual because they are typically only obtained from the reduction of Ag^+ in the presence of reducing agents such as $NaBH_4$ or $LiAlH_4$.[41] It has been reported that hydroxyl groups or alcoholic solution can reduce metal ions to zerovalent metals.[44,45] Thus, the residual hydroxyl groups on the esterified polyGMA chains may act as a reducing agent. To test this hypothesis, poly(acrylic acid)-functionalized MWNTs (MWNT-PAA)[24] were used to sequester Ag^+ ions, since the grafted poly(acrylic acid) chains do not contain any hydroxyl groups. However, similar silver nanoparticles were produced (Figure 14e). This comparative experiment suggests that the hydroxyl groups on the polyGMA chains do not play an essential role in the formation of silver nanoparticles. Further studies are planned in this area. In addition, Figure 14d,e indicates that the silver nanoparticles are enwrapped by the grafted polymer, which suggests that the carboxylic acid groups on the polymer chains sequester the metal ions prior to the formation of metallic aggregates. In comparison, no nanobead-like structure was observed for the CP3/La^{3+} nanocomposites (Figure 14f).

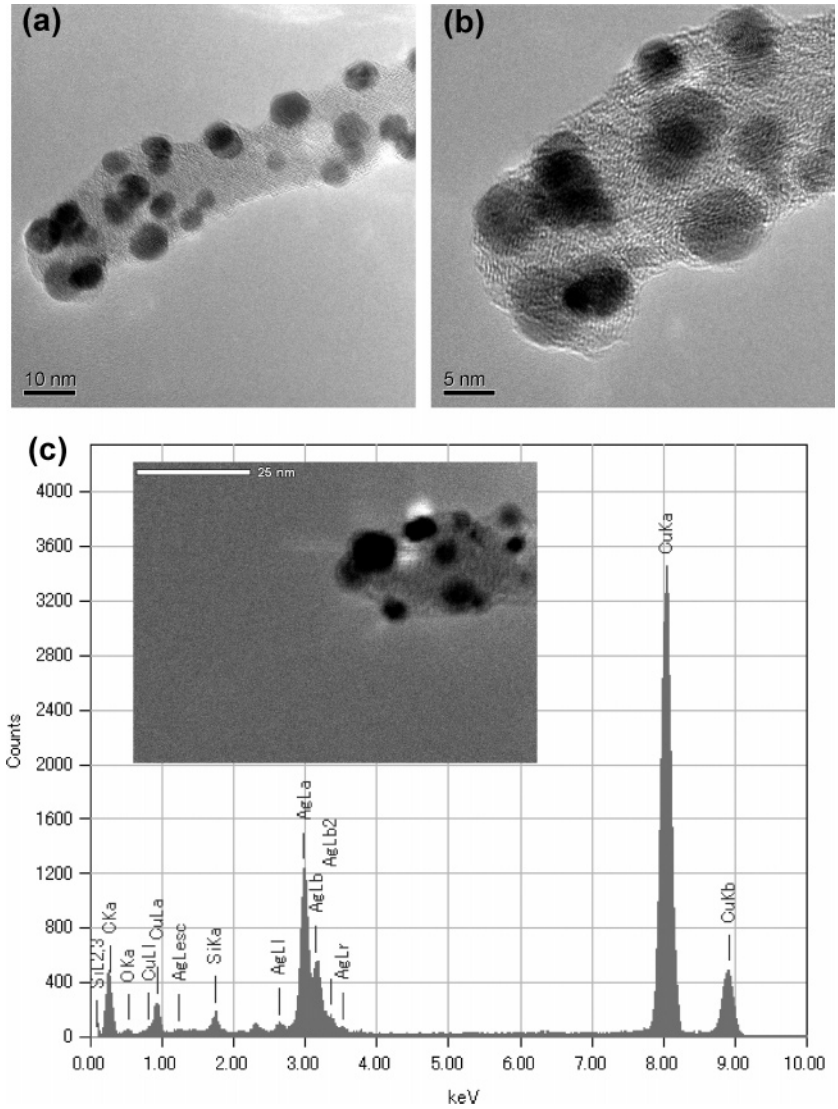

Figure 15. High-resolution transmission electron microscopy (HRTEM) images (a, b) and energy dispersive spectrum (EDS) (c) of a CP3b/Ag nanowire section. Inset of (c): EDS analyzing image.

The nanobead structure was further confirmed by HRTEM (Figure 15). Both single and twin nanobeads are observed by HRTEM with a diameter of ca. 5 nm (Figure 15a). Significantly, the crystalline lattice of some silver nanoparticles is apparent at higher magnification (Figure 15b), suggesting that these nanoparticles are either crystalline or semicrystalline. Electron diffraction (ED) studies of other MWNT-polymer/Ag samples also supported this observation (images not shown). Investigation of the formation of silver nanocrystals is in progress. The EDS measurements indicated relatively high silver contents (Figure 15c).

Conclusions

Multiwalled carbon nanotubes (MWNTs) were covalently functionalized with a hydrophilic hydroxylated polymer, polyGMA, by surface atom transfer radical polymerization (ATRP). The grafted polymer content can be efficiently controlled by the feed ratio of monomer to macroinitiator (MWNT-Br). Experiments with mixtures of MWNT-Br and soluble ethyl 2-bromoisobutyrate initiator showed that the molecular weight of the polymer increased monotonically as the monomer/initiator feed ratio was varied, while the polydispersity gradually broadened from ca. 1.5 to 3.75. This indicated that some of the chains became terminated during polymerizations in the presence of MWNT-Br. SEM and TEM observations showed that the nanotubes were coated with polymer chains. The resulting MWNT-polyGMA can form self-standing films providing that the level of grafted polymer is greater than 75%. The hydroxyl groups of the polyGMA chains grafted onto the MWNTs are still highly active and can be further reacted with succinic anhydride to be converted into carboxylic acid groups. The resulting carbon nanotubes can be aligned by self-assembly during solvent evaporation.

The derivatized polyacid-functionalized MWNTs can be used to sequester metal ions from aqueous solution. The extent of metal uptake can be adjusted by changing the proportion of metal ions relative to the functionalized MWNTs. For some metals such as cobalt and lanthanum, core−shell hybrid nanoobjects or nanocomposites can be prepared by such sequestration. Metals that can be easily reduced such as silver and gold allow the preparation of nanobead-like structures with a diameter of ca. 3−10 nm on the surface of the nanotubes. These nanobeads were tightly enwrapped by the polymer chains, forming stable necklace-like structures. These polyacid-functionalized CNTs have potential ap-

plications in the fields of water purification, metal separation, and new nanostructure fabrication.

TEM and Raman spectroscopy studies indicated that the carbon nanotube structure remained largely unchanged during chemical functionalization, polymer derivatization, and metal loading.

Acknowledgment. We acknowledge the financial support from the National Natual Sciences Foundation of China (Nos. 50473010 and 20304007), Fok Ying Tung Education Foundation (No. 91013), Rising-Star Program Foundation of Shanghai (No. 03QB14028), and EPSRC. We thank Prof. A. H. E. Müller and Dr. Mingfu Zhang of Bayreuth University (Germany) for good suggestions and helpful discussions.

References and Notes

(1) (a) Iijima, S. *Nature (London)* **1991**, *354*, 56−58. (b) Iijima, S.; Ichihashi, T. *Nature (London)* **1993**, *363*, 603−605.

(2) For example, see: (a) Liu, J.; Rinzler, A. G.; Dai, H. J.; Hafner, J. H.; Bradley, R. K.; Boul, P. J.; Lu, A.; Iverson, T.; Shelimov, K.; Huffman, C. B.; Rodriguez-Macias, F.; Shon, Y. S.; Lee, T. R.; Colbert, D. T.; Smalley, R. E. *Science* **1998**, *280*, 1253−1256. (b) Chen, J.; Hamon, M. A.; Hu, H.; Chen, Y.; Rao, A. M.; Eklund, P. C.; Haddon, R. C. *Science* **1998**, *282*, 95−98. (c) Ajayan, P. M. *Chem. Rev.* **1999**, *99*, 1787−1799. (d) Dai, H. *Acc. Chem. Res.* **2002**, *35*, 1035−1044. (e) Hirsch, A. *Angew. Chem., Int. Ed.* **2002**, *41*, 1853−1859. (f) Davis, J. J.; Coleman, K. S.; Azamian, B. R.; Bagshaw, C. B.; Green, M. L. H. *Chem.—Eur. J.* **2003**, *9*, 3732−3739. (g) Bianco, A.; Prato, M. *Adv. Mater.* **2003**, *15*, 1765−1768. (h) Lin, Y.; Taylor, S.; Li, H.; Fernando, S.; Qu, L.; Wang, W.; Gu, L.; Zhou, B.; Sun, Y.-P. *J. Mater. Chem.* **2004**, *14*, 527−541.

(3) (a) Sun, Y.-P.; Fu, K.; Lin, Y.; Huang, W. *Acc. Chem. Res.* **2002**, *35*, 1096−1104. (b) Niyogi, S.; Hamon, M. A.; Hu, H.; Zhao, B.; Bhowmik, P.; Sen, R.; Itkis, M. E.; Haddon, R. C. *Acc. Chem. Res.* **2002**, *35*, 1105−1113. (c) Wang, C. C.; Guo, Z. X.; Fu, S. K.; Wu, W.; Zhu, D. B. *Prog. Polym. Sci.* **2004**, *29*, 1079−1141.

(4) For example, see: (a) Hamon, M. A.; Chen, J.; Hu, H.; Chen, Y.; Itkis, M. E.; Rao, A. M.; Eklund, P. C.; Haddon, R. E. *Adv. Mater.* **1999**, *11*, 834−840. (b) Mickelson, E. T.; Chiang, I. W.; Zimmerman, J. L.; Boul, P. J.; Lozano, J.; Liu, J.; Smalley, R. E.; Hauge, R. H.; Margrave, J. L. *J. Phys. Chem. B* **1999**, *103*, 4318−4322. (c) Riggs, J. E.; Guo, Z.; Carroll, D. L.; Sun, Y.-P. *J. Am. Chem. Soc.* **2000**, *122*, 5879−5880. (d) Holzinger, M.; Vostrowsky, O.; Hirsh, A.; Hennrich, F.; Kappes, M.; Weiss, R.; Jellen, F. *Angew. Chem., Int. Ed.* **2001**, *40*, 4002−4005. (e) Kang, Y.; Taton, T. A. *J. Am. Chem. Soc.* **2003**, *125*, 5650−5651. (f) Carrillo, A.; Swartz, J. A.; Gamba, J. M.; Kane, R. S. *Nano Lett.* **2003**, *3*, 1437−1440. (g) Besteman, K.; Lee, J.-O.; Wiertz, F. G. M.; Heering, H. A.; Dekker, C. *Nano Lett.* **2003**, *3*, 727−730. (h) Rege, K.; Raravikar, N. R.; Kim, D.-Y.; Schadler, L. S.; Ajayan, P. M.; Dordick, J. S. *Nano Lett.* **2003**, *3*, 829−832. (i) Banerjee, S.; Kahn, M. G. C.; Wong, S. S. *Chem.—Eur. J.* **2003**, *9*, 1898−1908. (k) Gomez, F. J.; Chen, R. J.; Wang, D. W.; Waymouth, R. M.; Dai, H. J. *Chem. Commun.* **2003**, 190−191. (j) Tagmatarchis, N.; Prato, M. *J. Mater. Chem.* **2004**, *14*, 437−439. (k) Gao, C.; Jin, Y. Z.; Kong, H.; Whitby, R. L. D.; Acquah, S. F. A.; Chen, G. Y.; Qian, H. H.; Hartschuh, A.; Silva, S. R. P.; Henley, S.; Fearon, P.; Kroto, H. W.; Walton, D. R. M. *J. Phys. Chem. B* **2005**, *109*, 11925−11932.

(5) Sano, M.; Kamino, A.; Okamura, J.; Shinkai, S. *Langmuir* **2001**, *17*, 5125−5128.

(6) Kong, H.; Gao, C.; Yan, D. *J. Am. Chem. Soc.* **2004**, *126*, 412−413.

(7) Qin, S. H.; Qin, D. Q.; Ford, W. T.; Resasco, D. E.; Herrera, J. E. *Macromolecules* **2004**, *37*, 752−757.

(8) Liu, Y. Q.; Yao, Z. L.; Adronov, A. *Macromolecules* **2005**, *38*, 1172−1179.

(9) Qin, S. H.; Qin, D. Q.; Ford, W. T.; Herrera, J. E.; Resasco, D. E.; Bachilo, S. M.; Weisman, R. B. *Macromolecules* **2004**, *37*, 3965−3967.

(10) Koshio, A.; Yudasaka, M.; Zhang, M.; Iijima, S. *Nano Lett.* **2001**, *1*, 361−363.

(11) (a) Qu, L. W.; Lin, Y.; Hill, D. E.; Zhou, B.; Wang, W.; Sun, X. F.; Kitaygorodskiy, A.; Suarez, M.; Connell, J. W.; Allard, L. F.; Sun, Y. P. *Macromolecules* **2004**, *37*, 6055−6060. (b) Park, C.; Ounaies, Z.; Watson, K. A.; Crooks, R. E.; Smith, J.; Lowther, S. E.; Connell, J. W.; Siochi, E. J.; Harrison, J. S.; Clair, T. L. S. *Chem. Phys. Lett.* **2002**, *364*, 303−308.

(12) Lou, X. D.; Detrembleur, C.; Pagnoulle, C.; Jerome, R.; Bocharova, V.; Kiriy, A.; Stamm, M. *Adv. Mater.* **2004**, *16*, 2123−2127.

(13) (a) Riggs, J. E.; Guo, Z.; Carroll, D. L.; Sun, Y.-P. *J. Am. Chem. Soc.* **2000**, *122*, 5879−5880. (b) Riggs, J. E.; Walker, D. B.; Carroll, D. L.; Sun, Y.-P. *J. Phys. Chem. B* **2000**, *104*, 7071−7076.

(14) (a) Kahn, M. G. C.; Banerjee, S.; Wong, S. S. *Nano Lett.* **2002**, *2*, 1215−1218. (b) Huang, W.; Fernando, S.; Allard, L. F.; Sun, Y.-P. *Nano Lett.* **2003**, *3*, 565−568.

(15) Lin, Y.; Zhou, B.; Fernando, K. A. S.; Allard, L. F.; Sun, Y.-P. *Macromolecules* **2003**, *36*, 7199−7204.

(16) Zhao, B.; Hu, H.; Haddon, H. C. *Adv. Funct. Mater.* **2004**, *14*, 71−76.

(17) (a) Sun, Y.-P.; Huang, W.; Carroll, D. L. *Chem. Mater.* **2001**, *13*, 2864−2869. (b) Fu, K.; Huang, W.; Lin, Y.; Riddle, L. A.; Carroll, D. L.; Sun, Y.-P. *Nano Lett.* **2001**, *1*, 439−441.

(18) Sano, M.; Kamino, A.; Shinkai, S. *Angew. Chem., Int. Ed.* **2001**, *40*, 4661−4663.

(19) Cao, L.; Yang, W.; Yang, J.; Wang, C.; Fu, S. *Chem. Lett.* **2004**, *33*, 490−491.

(20) Kong, H.; Gao, C.; Yan, D. *Macromolecules* **2004**, *37*, 4022−4030.

(21) Baskaran, D.; Mays, J. W.; Bratcher, M. S. *Angew. Chem., Int. Ed.* **2004**, *43*, 2138−2142.

(22) Park, S. J.; Cho, M. S.; Lim, S. T.; Cho, H. J.; Jhon, M. S. *Macromol. Rapid Commun.* **2003**, *24*, 1070−1073.

(23) Yao, Z.; Braidy, N.; Botton, G. A.; Adronov, A. *J. Am. Chem. Soc.* **2003**, *125*, 16015−16024.

(24) Kong, H.; Luo, P.; Gao, C.; Yan, D. *Polymer* **2005**, *46*, 2472−2485.

(25) Qin, S.; Qin, D.; Ford, W. T.; Resasco, D. E.; Herrera, J. E. *J. Am. Chem. Soc.* **2004**, *126*, 170−176.

(26) Kong, H.; Gao, C.; Yan, D. *J. Mater. Chem.* **2004**, *14*, 1401−1405.

(27) Kong, H.; Li, W.; Gao, C.; Yan, D.; Jin, Y. Z.; Walton, D. R. M.; Kroto, H. W. *Macromolecules* **2004**, *37*, 6683−6686.

(28) Sun, T.; Liu, H.; Song, W.; Wang, X.; Jiang, L.; Li, L.; Zhu, D. *Angew. Chem., Int. Ed.* **2004**, *43*, 4663−4666.

(29) Qin, S. H.; Qin, D. Q.; Ford, W. T.; Herrera, J. E.; Resasco, D. E. *Macromolecules* **2004**, *37*, 9963−9967.

(30) Wu, W.; Zhang, S.; Li, Y.; Li, J. X.; Liu, L. Q.; Qin, Y. J.; Guo, Z. X.; Dai, L. M.; Ye, C.; Zhu, D. B. *Macromolecules* **2003**, *36*, 6286−6288.

(31) Xu, Y. Y.; Gao, C.; Kong, H.; Yan, D. Y.; Jin, Y. Z.; Watts, P. C. P. *Macromolecules* **2004**, *37*, 8846−8853.

(32) Save, M.; Weaver, J. V. M.; Armes, S. P.; McKenna, P. *Macromolecules* **2002**, *35*, 1152−1159.

(33) (a) Haigh, R.; Rimmer, S.; Fullwood, N. J. *Biomaterials* **2000**, *21*, 735−739. (b) Chen, Y. J.; Kang, E. T.; Neoh, K. G.; Tan, K. L. *Macromolecules* **2001**, *34*, 3133−3141. (c) Jones, D. M.; Brown, A. A.; Huck, W. T. S. *Langmuir* **2002**, *18*, 1265−1269. (d) Yu, W. H.; Kang, E. T.; Neoh, K. G. *Langmuir* **2004**, *20*, 8294−8300. (e) Wei, G.; Shirai, K.; Fujiki, K.; Saitoh, H.; Yamauchi, T.; Tsubokawa, N. *Carbon* **2004**, *42*, 1923−1929. (f) Murugan, R.; Ramakrishna, S. *Biomaterials* **2004**, *25*, 3073−3080.

(34) References related to ATRP, for example, see: (a) Pyun, J.; Kowalewski, T.; Matyjaszewski, K. *Macromol. Rapid Commun.* **2003**, *24*, 1043−1059. (b) Coessens, V.; Pintauer, T.; Matyjaszewski, K. *Prog. Polym. Sci.* **2001**, *26*, 337−377. (c) Pyun, J.; Matyjaszewski, K. *Chem. Mater.* **2001**, *13*, 3436−3448. (d) Matyjaszewski, K.; Xia, J. H. *Chem. Rev.* **2001**, *101*, 2921−2990. (e) Wang, J. S.; Matyjaszewski, K. *J. Am. Chem. Soc.* **1995**, *117*, 5614−5615. (f) Kato, M.; Kamigaito, M.; Sawamoto, M.; Higashimura, T. *Macromolecules* **1995**, *28*, 1721−1723.

(35) Bories-Azeau, X.; Mérian, T.; Weaver, J. V. M.; Armes, S. P.; van den Haak, H. J. W. *Macromolecules* **2004**, *37*, 8903−8910.

(36) Functional polymer brushes prepared by ATRP, for example, see: (a) Chen, X. Y.; Armes, S. P. *Adv. Mater.* **2003**, *15*, 1558−1562. (b) Chen, X. Y.; Armes, S. P.; Greaves, S. J.; Watts, J. F. *Langmuir* **2004**, *20*, 587−595. (c) Gao, C.; Qian, H.; Wang, S. B.; Kong, H.; Wang, S. J.; Yan, D. Y. *Acta Polym. Sin.* **2004**, *6*, 877−883. (d) Gao, C.; Qian, H.; Wang, S. B.; Kong, H.; Wang, S. J.; Yan, D. Y. *Acta Polym. Sin.* **2004**, *6*, 884−888. (e) Kong, X. X.; Kawai, T.; Abe, J.; Iyoda, T. *Macromolecules* **2001**, *34*, 1837−1844. (f) Borner, H. G.; Beers, K.; Matyjaszewski, K.; Sheiko, S. S.; Moller, M. *Macromolecules* **2001**,

34, 4375−4383. (g) Lord, S. J.; Sheiko, S. S.; LaRue, I.; Lee, H. I.; Matyjaszewski, K. *Macromolecules* **2004**, *37*, 4235−4240. (h) Mori, H.; Boker, A.; Krausch, G.; Müller, A. H. E. *Macromolecules* **2001**, *34*, 6871−6882. (i) Mori, H.; Seng, D. C.; Zhang, M. F.; Müller, A. H. E. *Langmuir* **2002**, *18*, 3682−3693. (j) Zhang, M. F.; Breiner, T.; Mori, H.; Müller, A. H. E. *Polymer* **2003**, *44*, 1449−1458.

(37) Matyjaszewski, K.; Miller, P. J.; Shukla, N.; Immaraporn, B.; Gelman, A.; Luokala, B. B.; Siclovan, T. M.; Kickelbick, G.; Vallant, T.; Hoffmann, H.; Pakula, T. *Macromolecules* **1999**, *32*, 8716−8724.

(38) Djalali, R.; Li, S. Y.; Schmidt, M. *Macromolecules* **2002**, *35*, 4282−4288.

(39) (a) Zhang, M. F.; Drechsler, M.; Müller, A. H. E. *Chem. Mater.* **2004**, *16*, 537−543. (b) Zhang, M. F.; Estournes, C.; Bietsch, W.; Müller, A. H. E. *Adv. Funct. Mater.* **2004**, *14*, 871−882.

(40) (a) Li, Y. H.; Ding, J.; Luan, Z. K.; Di, Z. C.; Zhu, Y. F.; Xu, C. L.; Wu, D. H.; Wei, B. Q. *Carbon* **2003**, *41*, 2787−2792. (b) Li, Y. H.; Wang, S. G.; Luan, Z. K.; Ding, J.; Xu, C. L.; Wu, D. H. *Carbon* **2003**, *41*, 1057−1062.

(41) Ma, R. Z.; Sasaki, T.; Bando, Y. *J. Am. Chem. Soc.* **2004**, *126*, 10382−10388.

(42) (a) Carrillo, A.; Swartz, J. A.; Gamba, J. M.; Kane, R. S.; Chakrapani, N.; Wei, B. Q.; Ajayan, P. M. *Nano Lett.* **2003**, *3*, 1437−1440. (b) Jiang, K. Y.; Eitan, A.; Schadler, L. S.; Ajayan, P. M.; Siegel, R. W.; Grobert, N.; Mayne, M.; Reyes-Reyes, M.; Terrones, H.; Terrones, M. *Nano Lett.* **2003**, *3*, 275−277. (c) Ellis, A. V.; Vjayamohanan, K.; Goswaimi, R.; Chakrapani, N.; Ramanathan, L. S.; Ajayan, P. M.; Ramanath, G. *Nano Lett.* **2003**, *3*, 279−282. (d) Fu, L.; Liu, Z. M.; Liu, Y. Q.; Han, B. X.; Wang, J. Q.; Hu, P. G.; Cao, L. C.; Zhu, D. B. *Adv. Mater.* **2004**, *16*, 350−352.

(43) Zhang, Y.; Franklin, N. W.; Chen, R. J.; Dai, H. J. *Chem. Phys. Lett.* **2000**, *331*, 35−41.

(44) Sun, X. M.; Li, Y. D. *Angew. Chem., Int. Ed.* **2004**, *43*, 597−601.

(45) (a) Mostafavi, M.; Dey, G. R.; François, L.; Belloni, J. *J. Phys. Chem. A* **2002**, *106*, 10184−10194. (b) Belloni, J.; Mostafavi, M.; Remita, H.; Marignier, J.-L.; Delcourt, M.-O. *New J. Chem.* **1998**, 1239−1255. (c) Dimitrijevic, N. M.; Bartels, D. M.; Jonah, C. D.; Takahashi, K.; Rajh, T. *J. Phys. Chem. B* **2001**, *105*, 954−959.

MA050823E